

# Deconfinement and criticality in extended two-dimensional dimer models

Anders W. Sandvik

*Department of Physics, Åbo Akademi University, Porthansgatan 3, FIN-20500 Turku, Finland*

(Dated: December 3, 2003)

A square-lattice hard-core dimer model with links extending beyond nearest-neighbors is studied using a directed-loop Monte Carlo method. An arbitrarily small fraction of next-nearest-neighbor dimers is found to cause deconfinement, whereas a critical state with  $r^{-2}$  distance dependence of the dimer-dimer correlations persists in the presence of longer dimers preserving the bipartite graph structure. However, the critical confinement exponent governing the correlation of two test monomers is non-universal. Implications for resonating-valence-bond states are discussed.

PACS numbers: 74.20.Mn, 75.10.-w, 05.10.Ln, 05.50.+q

Dimer models have a long history in classical statistical physics [1, 2, 3, 4]. More recently, they have also emerged as central models in modern theories of strongly correlated quantum matter, e.g., high-temperature cuprate superconductors and frustrated antiferromagnets [5, 6, 7, 8, 9, 10, 11]. The dimers then represent singlet-forming electron pairs. In order to model the quantum fluctuations of the dimers and realize a short-range version of Anderson's resonating valence bond (RVB) state [12, 13], Kivelson, Rokhsar, and Sethna introduced a Hamiltonian with a term flipping (resonating) pairs of parallel nearest-neighbor dimers on the two-dimensional (2D) square lattice [5]. The purely classical dimer model retains its relevance also here: It was shown that the equal-weight sum over all dimer configurations is the ground state of the Hamiltonian when the resonance strength  $-k$  equals the potential energy cost  $v$  of each resonating pair of dimers (the RK point) [6]. This state is critical; the dimer-dimer correlations decay with distance as  $r^{-2}$  and two inserted test monomers are correlated with each other as  $r^{-1/2}$  [4]. As it turned out, away from the RK point the dimers form long-range order and the monomers are exponentially confined [7, 14, 15]. Hence this system does not give rise to the desired RVB state with no broken lattice symmetries and deconfined monomers (corresponding to spin-charge separation [13]). Moessner and Sondhi recently showed that a true extended RVB phase *does* appear in the quantum dimer model on the triangular lattice [16]. Following this insight, a large body of work has been carried out in order to characterize classical and quantum dimer models on various lattices [9, 17, 18, 19, 20, 21]. Moreover, there are currently intense activities in gauge theories related to quantum dimer models [8, 9, 10, 11, 17, 22].

To date, research on dimer models has focused mainly on planar lattices, i.e., ones that have no intersecting links. This class of models can be analytically solved (in the form of Pfaffians) with the aid of a theorem by Kastelyn [3], and thus the quantum ground states at the corresponding RK points are characterized as well. It has often been stated that the inclusion of valence bonds (dimers) extending further than between

nearest-neighbor sites will not change the physics provided that the probability of longer bonds decreases sufficiently rapidly [6, 17]. However, the fact that there are qualitative differences between bipartite and nonbipartite lattices, e.g., the square and triangular cases mentioned above, does raise the question of potentially important effects of short bonds connecting two sites on the same sublattice of the square lattice. Such bonds will inevitably appear in realistic systems away from the limiting cases [5, 23, 24] represented by the nearest-neighbor ( $N_1$ ) dimer models. Introducing next-nearest-neighbor ( $N_2$ ) links along one of the diagonals makes the square lattice equivalent to the triangular one. It has already been shown that an arbitrarily small fraction of such diagonal dimers destroys the critical  $N_1$  square-lattice state and leads to deconfinement [11, 18], as in the isotropic triangular lattice [16]. The model with links along both diagonal directions, i.e., the full 2D square lattice with  $N_1$  and  $N_2$  bonds, is not solvable by Kastelyn's theorem [3]. Intuitively, one might suspect that the critical state is immediately destroyed in this case as well, but no calculations have been carried out thus far. One might also speculate that introducing longer bonds between the two sublattices does not lead to deconfinement, but there are no results available to back this up.

In this Letter, two extended dimer models on the square lattice are studied—the nonbipartite model with  $N_1$  and  $N_2$  dimers as well as the bipartite lattice with  $N_1$  and  $N_4$  (fourth-nearest-neighbors, of which there are eight per site). An efficient directed-loop [25] Monte Carlo algorithm is used to sample the full space of hard-core dimer configurations, with fugacities  $w_i$  assigned to the different dimer types. The results confirm that a low, most likely infinitesimal, concentration of  $N_2$  dimers leads to deconfinement, and that the presence of  $N_4$  dimers does not. However, while the dominant dimer correlations are  $\sim 1/r^2$  also when  $w_4 > 0$ , those correlations involve  $N_4$  dimers; the  $N_1$  correlations decay as a higher power of  $1/r$ . The structure in wave-vector space also becomes much more complicated. Furthermore, *the critical confinement exponent governing the monomer correlation function is nonuniversal*, changing continuously

from  $-1/2$  in the pure  $N_1$  case to  $-1/9$  (to high numerical accuracy) for the pure  $N_4$  model.

*Directed-loop algorithm.*—This algorithm is an adaptation of a quantum Monte Carlo method [25], with the same name, in which updates of the system degrees of freedom are carried out along a self-intersecting path at the endpoints of which there are defects not allowed in the configuration space contributing to the partition function. When the two defects meet they annihilate, the loop closes, and a new allowed configuration is created. The conditions for detailed balance in the process of stochastically moving one of the defects are expressed as a coupled set of *directed-loop equations* [25]. The applicability of this scheme to dimer models was first realized by Adams and Chandrasekharan [26] (an alternative cluster algorithm was constructed in Ref. [27]). Here an algorithm for the multi-length dimer problem will be presented; a simplifying representation of the dimer configurations will also be introduced. The algorithm will be described only for the case of the  $N_1$ - $N_2$  model, but the scheme applies directly to any range of the links.

The links connected to a given site are labeled as shown in Fig. 1(a). For a dimer configuration on a periodic  $L \times L$  lattice, each site is numbered according to the type of dimer it is connected to. For any given site, the other member of the same dimer can then be easily found. The central object in the directed-loop algorithm is a *vertex*, which in this case consists of a site and all its surrounding sites to which it can be coupled by a dimer. The state of the vertex is the number (1-8) assigned to the central site. A step in the directed-loop algorithm is illustrated in Fig. 1(b). The vertex is entered through the dimer, and one of the seven other surrounding sites is chosen as the exit. The dimer is then flipped from the entrance to the exit, the central vertex site remaining connected to it. The exit site already has another dimer connected to it, and this site now becomes the entrance in the next step of the algorithm. In each step a defect is hence moved one link ahead, leaving behind a healed dimer state. The first entrance site is chosen at random and the corresponding defect remains stationary. It is annihilated when the moving defect reaches it, whence a new allowed dimer configuration has been generated. In the present case the defects are monomers, and the intermediate two-monomer configurations can thus be used to measure the correlations between two inserted test monomers.

The key to an efficient algorithm of this kind is that the probabilities for random selection of the seven possible exit sites can be chosen in such a way that detailed balance is satisfied without any further accept/reject criterion. Each step then moves one dimer, and a full loop can accomplish very significant changes to the dimer configuration. The directed-loop equations [25] give the conditions for detailed balance in terms of weights  $a_{jk}$  for the processes in which a vertex in state  $j$  is entered at site  $j$  and exited at  $k$  (transforming the vertex into state

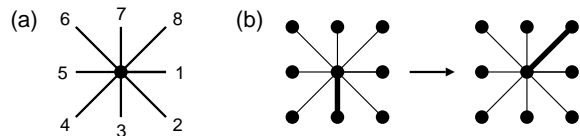


FIG. 1: (a) Labeling of the links of the  $N_1$ - $N_2$  dimer model. (b) A step in the directed-loop update, in which the entrance to the vertex is at site 3 and the exit is at site 8. The thick bond indicates the location of the dimer.

$k$ ). The actual probabilities  $P_{jk} = a_{jk}/w_j$ , which implies  $\sum_k a_{jk} = w_j$ . Detailed balance is satisfied if  $a_{jk} = a_{kj}$ . In the  $N_1$ - $N_2$  model, the vertices can be classified as even ( $e$ ) or odd ( $o$ ) according to the numbering of Fig. 1(a); there are then four weights:  $a_{ee}, a_{oo}, a_{eo}, a_{oe}$ . In principle, one can include “bounce” processes where  $j = k$ , but in the present case they can be excluded. Including only the seven no-bounce exits, the directed-loop equations reduce to

$$w_1 = 3a_{oo} + 4a_{oe}, \quad (1a)$$

$$w_2 = 3a_{ee} + 4a_{eo}, \quad (1b)$$

$$a_{eo} = a_{oe}. \quad (1c)$$

This system is underdetermined and has an infinite number of positive-definite solutions. Here the following solution will be used: For  $w_1 \geq w_2$ ,

$$a_{ee} = a_{oe} = a_{eo} = w_2/7, \quad (2a)$$

$$a_{oo} = (w_1 - 4w_2/7)/3, \quad (2b)$$

while for  $w_2 \geq w_1$ ,

$$a_{oo} = a_{oe} = a_{eo} = w_1/7, \quad (3a)$$

$$a_{ee} = (w_2 - 4w_1/7)/3. \quad (3b)$$

There is no guarantee that this is the best solution, but the resulting algorithm performs very well and allowed for studies of lattices with  $\sim 10^6$  dimers. The fugacity of the  $N_1$ -bonds is set to unity (except in the case of the pure  $N_2$ - and  $N_4$ -models). The program was tested using known results for the pure  $N_1$  case [4] and by comparing with local Metropolis simulations for small lattices.

*Results.*—Dimer-dimer correlations in the full close-packed system and monomer-monomer correlations in the system with two test monomers will be discussed. The monomer correlations  $M(\mathbf{r})$  were obtained by accumulating the distances between the stationary and the moving monomer in the directed-loop update. As has become customary [27], the normalization  $M(r=1) = 1$ . Several types of dimer-dimer correlations can be defined. Here  $D_\Sigma(\mathbf{r})$  will be defined in the following way: If site  $i$  is connected to a dimer in the set  $\Sigma$ , a variable  $s(i) = 1$ , otherwise  $s(i) = 0$ . The correlation function is then  $D_\Sigma(\mathbf{r}_{ij}) = \langle s(i)s(j) \rangle$ . Results will be presented for cases where  $\Sigma$  contains a single dimer or half of the dimers of

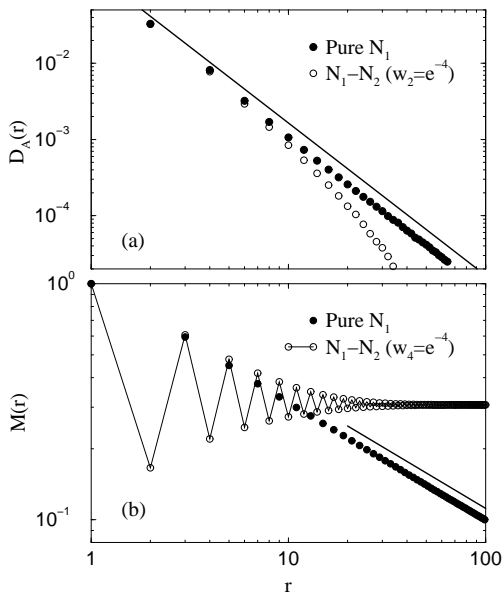


FIG. 2: Dimer (a) and monomer (b) correlations along the direction  $(r, 0)$  for the  $N_1-N_2$  model at  $w_2 = e^{-4}$ , compared with those of the pure  $N_1$  model. The solid lines show the agreement with the known power-laws [4] for the  $N_1$  model. Note that for the pure  $N_1$  model  $M(r) = 0$  for even  $r$ . The results were obtained using  $L = 1024$  lattices.

one type. For the  $N_1-N_2$  model, the correlation functions  $D_1$ ,  $D_2$ ,  $D_A$ , and  $D_B$  are thus defined corresponding to the sets  $\{1\}$ ,  $\{2\}$ ,  $A = \{1, 3\}$ , and  $B = \{2, 4\}$ . Analogous definitions are used for correlations  $D_1$ ,  $D_A$  of  $N_1$  dimers and  $D_4$ ,  $D_D$  of  $N_4$  dimers in the  $N_1-N_4$  model.

In Fig. 2(a), dimer correlations  $D_A$  for the nonbipartite  $N_1-N_2$  model with  $w_2 = e^{-4}$  (corresponding to a concentration  $p_2 \approx 0.3\%$  of  $N_2$  dimers) are compared with those of the pure  $N_1$  model. There is a clear deviation from the  $r^{-2}$  decay, showing that the  $N_1-N_2$  model is not critical at this very low concentration of  $N_2$  dimers. As shown in Fig. 2(b), the test monomer correlation approaches a nonzero constant, i.e., the system is deconfined in contrast to the critically confined  $N_1$  model. The very significant changes seen already at a very low concentration of  $N_2$  dimers suggest that an arbitrarily small concentration indeed causes deconfinement.

Turning now to the bipartite  $N_1-N_4$  model, its dimer correlations  $D_A(r)$  ( $N_1$  dimers) and  $D_D(r)$  ( $N_4$  dimers) are compared with  $D_A(r)$  of the pure  $N_1$  model in Fig. 3. Surprisingly, the two correlation functions decay with different power-laws:  $D_D(r)$  apparently always follows the same form  $r^{-2}$  as  $D_A(r)$  of the pure  $N_1$  model, whereas  $D_A(r)$  decays faster once  $w_4 > 0$ . In Fig. 4 the Fourier transforms of the correlation functions involving a single type of dimer are shown for the pure  $N_1$  and  $N_4$  models. For the  $N_1$  model, the dominant correlations are at  $\mathbf{q} = (\pi, 0)$ . A logarithmic divergence of the peak height with the system size can easily be observed (not shown

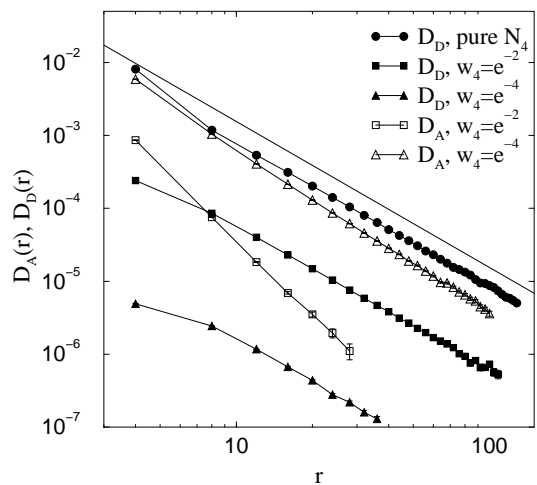


FIG. 3: Various dimer correlations along the direction  $(r, 0)$  in the  $N_1-N_4$  model (on  $L = 1024$  lattices). The fugacities  $w_4 = e^{-4}$  and  $e^{-2}$  correspond to concentrations  $p_4 \approx 0.065$  and  $0.17$ , respectively. The solid line shows the asymptotic form  $r^{-2}$ .

here). The  $N_4$  model exhibits more complicated correlations, with very broad peaks that show almost no size dependence up to the largest size ( $L = 2048$ ) that was studied. Nevertheless, a logarithmic divergence should eventually occur here as well, considering the  $r^{-2}$  real-space correlations. The details of the nature of these critical correlations remain to be elucidated. In the  $N_1-N_4$  model, the wave-vector structures shown in Fig. 4 change with  $w_4$ . Most notably, the  $D_1$  peak at  $(\pi, 0)$  is suppressed as the fraction of  $N_4$  dimers increases, and a nondivergent structure at  $(\pi, \pi)$  emerges.

An unchanged dominant critical dimer exponent might suggest that the monomer correlations should also remain of the pure  $N_1$  form  $r^{-1/2}$ . This is not the case, however. Results for  $M(r)$  at  $r = L/2 - 1$  are shown multiplied by  $L^\alpha$  in Fig. 5(a). Here  $\alpha$  is adjusted to give a flat  $L$  dependence, and hence the critical form  $M(r) \sim r^{-\alpha}$  is extracted. The known  $\alpha = 1/2$  is used for the pure  $N_1$  model. For the pure  $N_4$  model the exponent is consistent with  $\alpha = 1/9$  (to an accuracy of 1%). To show that the exponent changes from  $1/2$  already at a low concentration of  $N_4$  bonds, results for  $w_4 = e^{-5}$  ( $p_4 \approx 0.9\%$ ) are scaled with  $\alpha = 1/2$  in Fig. 5(b). This scaling clearly fails, and is instead consistent with  $\alpha \approx 0.485$ .

*Conclusions.*—The results obtained here demonstrate that the 2D square-lattice dimer model becomes deconfined when a very low concentration (likely infinitesimal) of non-bipartite (next-nearest-neighbor) dimers are introduced. The system remains critically confined in the presence of longer bipartite (fourth-nearest-neighbor) dimers, but the corresponding two-monomer exponent is nonuniversal. In contrast, the dimer-dimer correlation exponent appears to remain unchanged, although the na-

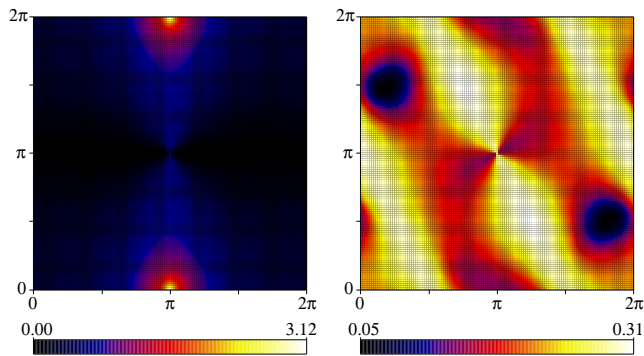


FIG. 4: Fourier transform of the dimer-dimer correlation  $D_1$  of the  $N_1$  model (left) and  $D_4$  of the  $N_4$  model (right) calculated on  $L = 128$  lattices.

ture of the dominant correlations changes.

These findings are relevant to quantum dimer models as well. Various resonance terms can be introduced, and corresponding RK points can then be demonstrated in the same way as has been done for other models [6, 11, 28]. Hence, it is clear that an RVB state can be realized on the square lattice once next-nearest-neighbor dimers are allowed. On the other hand, the emergence of new structure in the dominant dimer-dimer correlations on the bipartite graph including fourth-nearest-neighbor links indicates that phase transitions between different long-range ordered valence-bond-solid states can be realized. Such quantum order-order transitions have recently been discussed by Vishwanath, Balents, and Senthil [22]. Extended quantum dimer models on the square lattice should thus have very rich phase diagrams and may also be relevant in the context of the cuprates.

This work was supported by the Academy of Finland, Project No. 26175. The calculations were carried out on the Condor system at the University of Wisconsin-Madison.

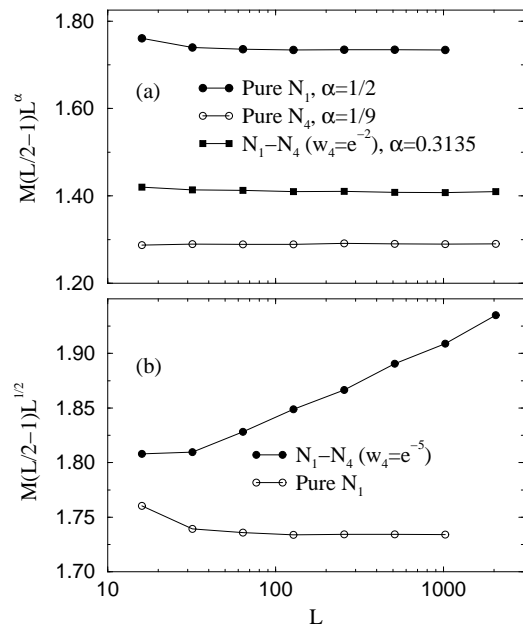


FIG. 5: Finite-size scaling of monomer correlations in the  $N_1$ - $N_4$  model. (a) The best scaling for three different cases. (b) Failure of a scaling with the pure  $N_1$  exponent  $\alpha = 1/2$  for the  $N_1$ - $N_4$  model at low fugacity  $w_4$ .

[1] R. H. Fowler and G. S. Rushbrooke, *Trans. Faraday Soc.* **33**, 1272 (1937).  
 [2] M. E. Fisher, *Phys. Rev.* **124**, 1664 (1961).  
 [3] P. W. Kastelyn, *Physica* **27**, 1209 (1961); *J. Math. Phys.* **4**, 287 (1963).  
 [4] M. E. Fisher and J. Stephenson, *Phys. Rev.* **132**, 1411 (1963).  
 [5] S. A. Kivelson, D. S. Rokhsar, and J. P. Sethna, *Phys. Rev. B* **35**, 8865 (1987).  
 [6] D. S. Rokhsar and S. A. Kivelson, *Phys. Rev. Lett.* **61**, 2376 (1988).  
 [7] E. Fradkin, *Field theories of condensed matter systems* (Addison-Wesley, Redwood City 1991).  
 [8] T. Senthil and M. P. A. Fisher, *Phys. Rev. B* **62**, 7850 (2000).  
 [9] G. Misguich, D. Serban, and V. Pasquier, *Phys. Rev. Lett.* **89**, 137202 (2002).

[10] S. Sachdev, *Rev. Mod. Phys.* **75**, 913 (2003).  
 [11] E. Ardonne, P. Fendley, and E. Fradkin, *cond-mat/0311466*.  
 [12] P. W. Anderson, *Mater. Res. Bull.* **8**, 153 (1973); P. Fezekas and P. W. Anderson, *Philos. Mag.* **30**, 23 (1974).  
 [13] P. W. Anderson, *Science* **235**, 1196 (1987).  
 [14] S. Sachdev, *Phys. Rev B* **40**, 5204 (1989).  
 [15] P. W. Leung, K. C. Chiu, and K. J. Runge, *Phys. Rev. B* **54**, 12938 (1996).  
 [16] R. Moessner and S. L. Sondhi, *Phys. Rev. Lett.* **86**, 1881 (2001).  
 [17] R. Moessner and S. L. Sondhi, and E. Fradkin, *Phys. Rev. B* **65**, 024504 (2001).  
 [18] P. Fendley, R. Moessner, and S. L. Sondhi, *Phys. Rev. B* **66**, 214513 (2002).  
 [19] D. A. Huse, W. Krauth, R. Moessner, and S. L. Sondhi, *Phys. Rev. Lett.* **91**, 167004 (2003).  
 [20] R. Moessner and S. L. Sondhi, *Phys. Rev. B* **68**, 054405 (2003).  
 [21] E. Fradkin, D. A. Huse, R. Moessner, V. Oganesyan, and S. L. Sondhi, *cond-mat/0311353*.  
 [22] A. Vishwanath, L. Balents, T. Senthil, *cond-mat/0311085*.  
 [23] J. T. Chayes, L. Chayes, and S. A. Kivelson, *Commun. Math. Phys.* **123**, 53 (1989).  
 [24] N. Read and S. Sachdev, *Nucl. Phys. B* **316**, 609 (1989).  
 [25] O. F. Syljuåsen and A. W. Sandvik, *Phys. Rev. E* **66**, 046701 (2002).  
 [26] D. H. Adams and S. Chandrasekharan, *Nucl. Phys. B* **662**, 220 (2003).  
 [27] W. Krauth and R. Moessner, *Phys. Rev. B* **67**, 064503 (2003).  
 [28] C. L. Henley, *cond-mat/0311345*.